Computational Study of Magnetic Islands in the W7-X and NCSX Stellarators

M. Drevlak 1), C. Nührenberg 1), A.H. Boozer 2), S.R. Hudson 2), L.P. Ku 2), D. Monticello 2), A. Reiman 2)

1) IPP-Euratom Association, MPI für Plasmaphysik, 17491 Greifswald, Germany
2) Princeton Plasma Physics Laboratory, PO Box 451, Princeton NJ 08543, USA

e-mail contact of main author: Michael.Drevlak@ipp.mpg.de

Abstract. The magnetic fields of stellarators and, in general, all not strictly axisymmetric toroidal fusion devices exhibit magnetic islands. Codes that determine finite-plasma-β stellarator equilibria while fully accounting for their island structures exist. Equilibria obtained for the National Compact Stellarator Experiment (NCSX) and the Wendelstein 7-X stellarator using the Princeton Iterative Equilibrium Solver (PIES) code are presented. An alternative approach to the assessment of magnetic islands in finite-β stellarator equilibria has been developed with the method of perturbed equilibria. Since a perturbed equilibrium represents a small deviation from an equilibrium, it can be determined by ideal magnetohydrodynamic (MHD) stability theory and ideal MHD stability codes, e.g. the Code for the Analysis of 3-dimensional Equilibria (CAS3D). Discontinuities of the normal displacement at rational surfaces indicate surface currents which are used to model islands: the strength of such a surface current can be used to estimate the corresponding island width. The alternative method to determine islands within ideal MHD was implemented in the CAS3D code and yields island sizes comparable to the ones given by the PIES code.

1. Introduction

The magnetic fields of stellarators and, in general, all not strictly axisymmetric toroidal fusion devices exhibit magnetic islands. They strongly influence the confinement properties and are exploited in divertor design. So, the existence and the structure of the magnetic islands are an important issue in configuration design. In stellarators there are two types of islands. *Intrinsic* islands are caused by the stellarator shaping fields. Their toroidal mode number is a multiple of the number of stellarator field periods. On the other hand, *error-field*-induced islands can have any toroidal mode number. In tokamaks, only the latter type of islands exists.

Codes that determine finite-plasma-β stellarator equilibria while fully accounting for their island structures exist, but have only been applied to intrinsic islands up to now owing to the otherwise larger computational effort. The Princeton Iterative Equilibrium Solver (PIES) [1] and the HINT code [2] are of particular importance for stellarator applications.

From the theory of perturbed equilibria a different method has been developed to study islands in stellarator plasmas [3] and has been implemented in the Code for the Analysis of 3-dimensional Equilibria (CAS3D) [4].

For the study presented here, both approaches have been applied to the National Compact Stellarator Experiment (NCSX) [5] and the Wendelstein 7-X (W7-X) stellarator [6]. The purpose of this paper is to describe both methods and to present numerical calculations with a comparison of the results.

2. The PIES Code

The PIES code (Princeton Iterative Equilibrium Solver) [1] solves for stellarator symmetric MHD equilibria defined by

$$\vec{\jmath} \times \vec{B} = \nabla p, \qquad \nabla \times \vec{B} = \mu_0 \vec{\jmath}, \qquad \nabla \cdot \vec{B} = 0. \tag{1}$$

Contrary to the VMEC code (Variational Moments Equilibrium Code) [7], where the plasma volume is fixed by input parameters and flux surfaces are assumed, PIES makes no a priori assumption about the existence of closed flux surfaces.

Any computation of the magnetic induction, $\vec{B}$, requires knowledge of the current density, $\vec{\jmath}$. The spatial structure of $\vec{\jmath}$, in turn, depends on the existence and integrity of flux surfaces of $\vec{B}$. As there is no simple way to determine a priori whether a field line launched from any starting point forms a closed flux surface, a magnetic island or behaves stochastically, PIES employs a Picard iteration to obtain a solution for Eq. (1). This approach was proposed in Ref. [8]. During each iteration, i, PIES computes the spatial distribution of the current density, $\vec{\jmath}(\vec{B}^i)$. Then the current density is used to compute the new magnetic field:

$$\nabla \times \vec{B}^{i+1} = \mu_0 \vec{\jmath}(\vec{B}^i). \tag{2}$$

Unfortunately, the unmodified iteration (2) is observed to be unstable for plasma pressures of relevant magnitude. Therefore, convergence is established by blending quantities of the latest iteration with those of the preceding one.

$$\vec{B}^{i+1} = (1-b) \cdot \vec{B}(\vec{\jmath}^{\,i}) + b \cdot \vec{B}^i, \tag{3}$$

where b is a blending parameter.

For W7-X [6] cases like the one presented in this publication, with $\langle\beta\rangle \geq 4\%$ and large numbers of Fourier modes (m=10 poloidal, n=8 toroidal) describing equilibrium quantities, large values, typically $b = 0.99\ldots0.999$, are needed for the blending parameter. It follows that the rate of convergence is reduced and some 10^2 to 10^3 iterations are required before a sufficiently converged solution is obtained.

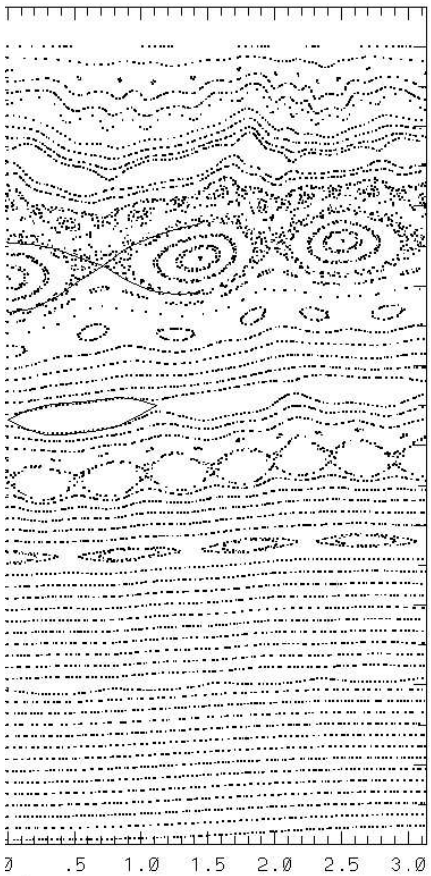

Figure 1: *Poincaré plot showing the upper half of the triangular cross-section of an NCSX finite-β fixed-boundary PIES calculation,* $\langle\beta\rangle = 0.04$.

3. PIES Calculations

3.1. NCSX

In the NCSX standard high-β scenario low-order rotational-transform values exist inside the plasma [9]. A

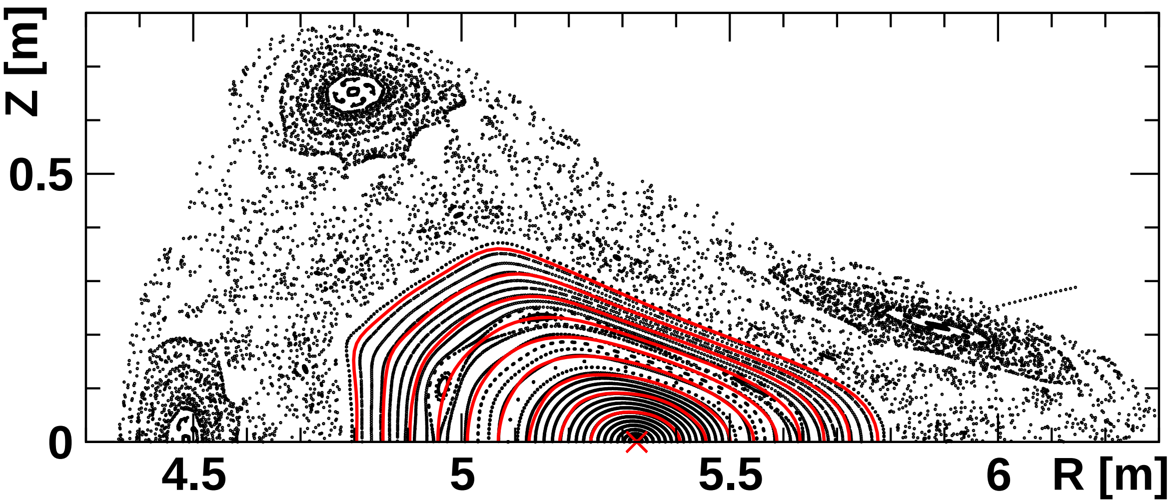

Figure 2: *Poincaré plot showing the upper half of the triangular cross-section of a W7-X finite-β PIES calculation, $\langle\beta\rangle = 0.05$. Flux surfaces from a VMEC calculation are shown in red.*

fixed-boundary PIES calculation for an NCSX-type case at $\langle\beta\rangle = 0.04$ has a very similar magnetic topology, see Fig. 1 with half of a poloidal cut for this case in the $(\vartheta, r_\mathrm{n})$ plane. Here, $0 \leq \vartheta \leq 2\pi$ is a poloidal angle, and $0 \leq r_\mathrm{n} \leq 1$ a normalized radius. Several $3/m$ and $6/m$ islands can be seen, e.g. $3/5$ and $3/6$ in this 3-periodic device.

3.2. W7-X

For the 5-periodic W7-X stellarator the situation is different: In the standard high-β case no low-order rationals exist inside the plasma. However, W7-X will be equipped with independently powered primary field coils and with planar auxiliary coils. These features will allow W7-X to access operating regimes with increased or reduced rotational transform as well as enhanced or reduced mirror component of the magnetic field and an inward or outward shift of the magnetic axis [10].

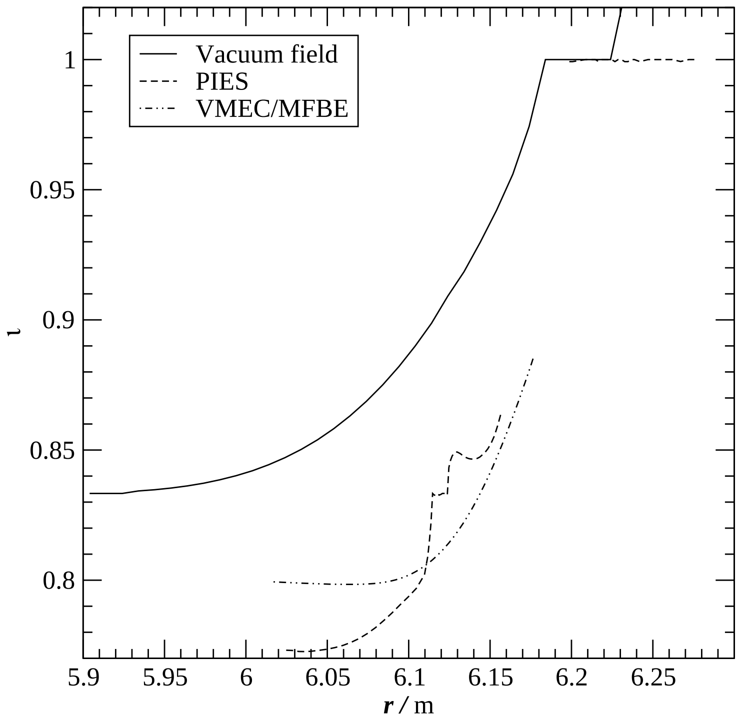

Figure 3: *W7-X: ι profiles of the vacuum field (solid line), the VMEC equilibrium obtained from the MFBE procedure (dash-dot-dot) and from the PIES calculation (dashed, compare Fig. 2). ι is plotted versus the starting point of the field line at the bean-shaped cross-section. Note that at finite β the axis is shifted outward by ≈ 0.11 m. It can be seen that the plasma volume is reduced significantly by the introduction of finite plasma pressure.*

This implies that equilibria with low order rationals inside the confinement region are in principle possible. The equilibrium calculation presented in [11], although free of significant internal islands, depends on the capability to adjust the magnetic field. Recently, the PIES code was used to obtain a free boundary equilibrium at $\langle\beta\rangle = 5\%$ which exhibits a chain of $\iota = 5/6$ islands inside the plasma (see Fig. 2). In calculations using the **M**agnetic **F**ield Solver for Finite-**B**eta **E**quilibria (MFBE) [12] preceding the PIES computation, a configuration of coil currents was selected similar to one previously successful at $\beta = 4\%$ [11]. This configuration employs the auxiliary coils, energised so as to increase the confinement volume of the vacuum field by shifting the magnetic axis inward and adjusting the ι profile.

The plasma volume is reduced from 35.2m^3 in the vacuum field to $\sim$ 15m^3 at $\langle\beta\rangle = 5\%$. the iota profile of both the vacuum and the finita β fields computed by VMEC and PIES are shown in Fig. 3

The computation was carried out with 10 poloidal and 8 toroidal modes on $N = 70$ radial surfaces. A total of 6200 iterations was used in the final coordinate system.

4. Perturbed Equilibrium Method

An alternative approach to the assessment of magnetic islands in finite-β stellarator equilibria has been developed with the method of perturbed equilibria [3]. Since a perturbed equilibrium represents a small deviation from an equilibrium, it can be determined by ideal magnetohydrodynamic (MHD) stability theory and ideal MHD stability codes. For tokamak geometry this concept has been used in the IPEC code [13]. For general geometry and, hence, suitable for the study of stellarator cases, the procedure was implemented in the CAS3D code [4].

An initial plasma state, not necessarily in equilibrium, is given by a set of surfaces, together with the rotational transform, ι, and pressure, p, profiles. The VMEC 3d ideal MHD equilibrium code [7] is used here. This code assumes nested surfaces. The obtained data is mapped to magnetic coordinates (s,θ,ϕ), with the magnetic field $\vec{B}$ representation

$$\vec{B} = I\nabla\phi + J\nabla\theta + \widetilde{\beta}\nabla s = -\frac{F_{\mathrm{T}}'}{\sqrt{g}}\vec{r}_{,\phi} - \frac{F_{\mathrm{P}}'}{\sqrt{g}}\vec{r}_{,\theta} \quad . \tag{4}$$

In Eq. (4), the poloidal (toroidal) currents are denoted by I (J); the poloidal (toroidal) fluxes are F_{P} (F_{T}). Primes denote derivatives of flux surface functions, $f' = \mathrm{d}f/\mathrm{d}s$. The Jacobian is $\sqrt{g}$. The covariant component $\widetilde{\beta}$ may be determined from the metric coefficients as $\sqrt{g}\widetilde{\beta}_{\mathrm{metric}} = F_{\mathrm{T}}' g_{s\phi} + F_{\mathrm{P}}' g_{s\theta}$. For an equilibrium state the ideal MHD force balance holds, $\nabla p = \vec{\jmath}\times\vec{B}$, Eq. (1). The quantity $\widetilde{\beta}_{\mathrm{mde}}$ is defined by the magnetic differential equation $\sqrt{g}\vec{B}\cdot\nabla\widetilde{\beta}_{\mathrm{mde}} = p'(\sqrt{g}-V')$ derived from its scalar analog in magnetic coordinates. An equilibrium requires $\widetilde{\beta}_{\mathrm{metric}} = \widetilde{\beta}_{\mathrm{mde}}$.

A perturbed equilibrium is described by

$$\nabla(p+\delta p) = (\vec{\jmath}+\delta\vec{\jmath})\times(\vec{B}+\delta\vec{B}) \quad , \tag{5}$$

and by the stationarity of the variation

$$\delta W = \delta^1 W + \delta^2 W = \int(\nabla p - \vec{\jmath}\times\vec{B})\cdot\vec{\xi}\ \mathrm{d}^3 r - \frac{1}{2}\int\vec{\xi}\cdot\mathscr{F}\left[\vec{\xi}\right]\mathrm{d}^3 r \quad . \tag{6}$$

In Eq. (6) $\mathscr{F}$ is the ideal MHD force operator. The first order variation, $\delta^1 W$, can be rewritten as [14]

$$\delta^1 W = \int \xi^s \left\{(p' - p_{\mathrm{n}}') + \vec{B}\cdot\nabla(\widetilde{\beta}_{\mathrm{mde}} - \widetilde{\beta}_{\mathrm{metric}})\right\}\mathrm{d}^3 r \quad . \tag{7}$$

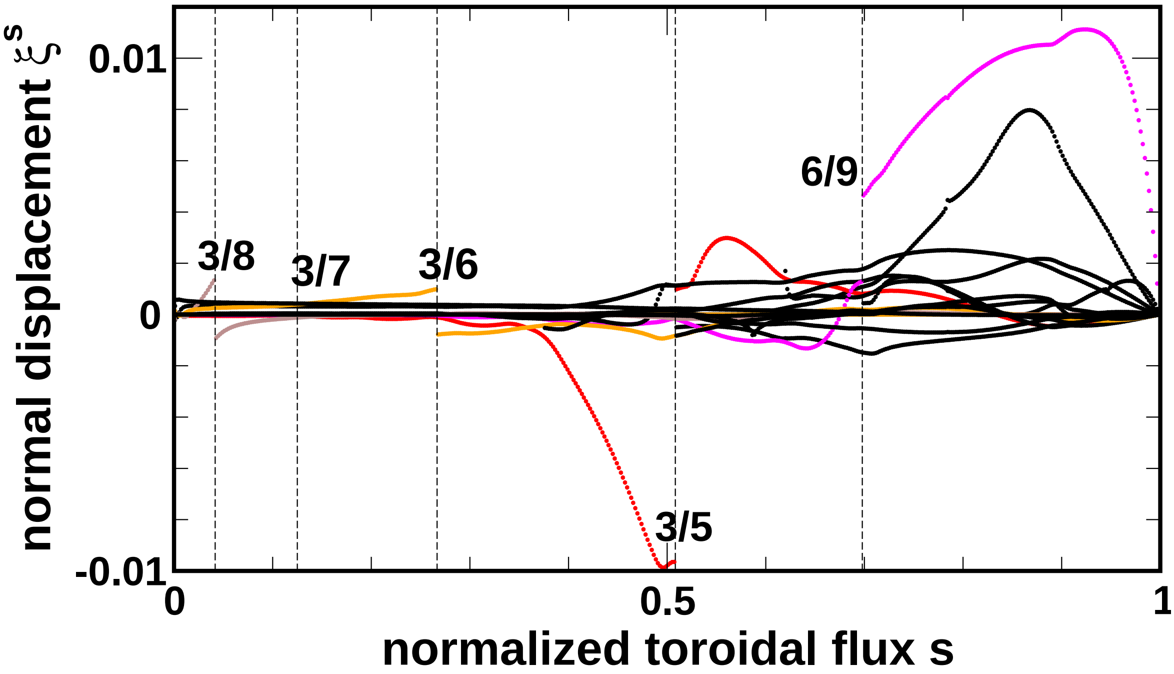

Figure 4: *CAS3D result for the NCSX-type case of Fig. 1: The dominant normal displacement harmonics versus normalized toroidal flux s. Resonant harmonics (coloured lines) may jump at their respective rational surfaces (dashed). The rational ι values are given.*

For a plasma state with islands, the VMEC result is a set of surfaces that does not describe an MHD equilibrium in the vicinity of the islands. Then the second term in $\delta^1 W$ describes the departure of this plasma state, described by $\widetilde{\beta}_{\mathrm{metric}}$, from an equilibrium for which $\widetilde{\beta}_{\mathrm{metric}} = \widetilde{\beta}_{\mathrm{mde}}$ must hold. If the plasma-pressure is slightly changed, then the first term also contributes. For a given plasma geometry the equation $p_{\mathrm{n}}' V' = I' F_{\mathrm{T}}' + J' F_{\mathrm{P}}'$ determines the plasma pressure p_{n} which is compatible with the MHD equilibrium condition, Eq. (1).

In CAS3D δW is made stationary with a Galerkin method giving a set of linear equations. The RHS $\vec{g}$ is given by $\delta^1 W$, the system matrix by $\delta^2 W$. For the perturbed equilibrium one may write

$$\mathscr{F}\left[\vec{\xi}\right] = \vec{g} \quad . \tag{8}$$

The boundary conditions for the normal displacement, $\xi^s = \vec{\xi} \cdot \nabla s$, used with Eq. (8) determine the type of perturbed equilibrium. In a study of stellarator intrinsic islands $\xi^s(\mathrm{boundary}) \equiv 0$ is chosen, which means that the plasma boundary is not perturbed. In the case of a perturbed boundary-shape or external field the normal displacement is prescribed a finite value on the plasma boundary, $\xi^s(\mathrm{boundary}) \neq 0$.

In either case, resonant error fields produce islands. In ideal MHD, a surface current, $\vec{\jmath}_{\mathrm{surf}}$, is employed on the rational surface which prevents an island from opening,

$$\begin{aligned} \vec{n} \cdot \left[\delta \vec{B}\right] &= 0 \\ \vec{n} \times \left[\delta \vec{B}\right] &= \mu_0 \, \vec{\jmath}_{\mathrm{surf}} \quad . \end{aligned} \tag{9}$$

So, the augmented CAS3D code allows for a generalized class of MHD eigenfunctions which may have jumps in resonant normal displacement harmonics on the respective rational surface. The discontinuities of the normal displacement at rational surfaces indicate surface currents

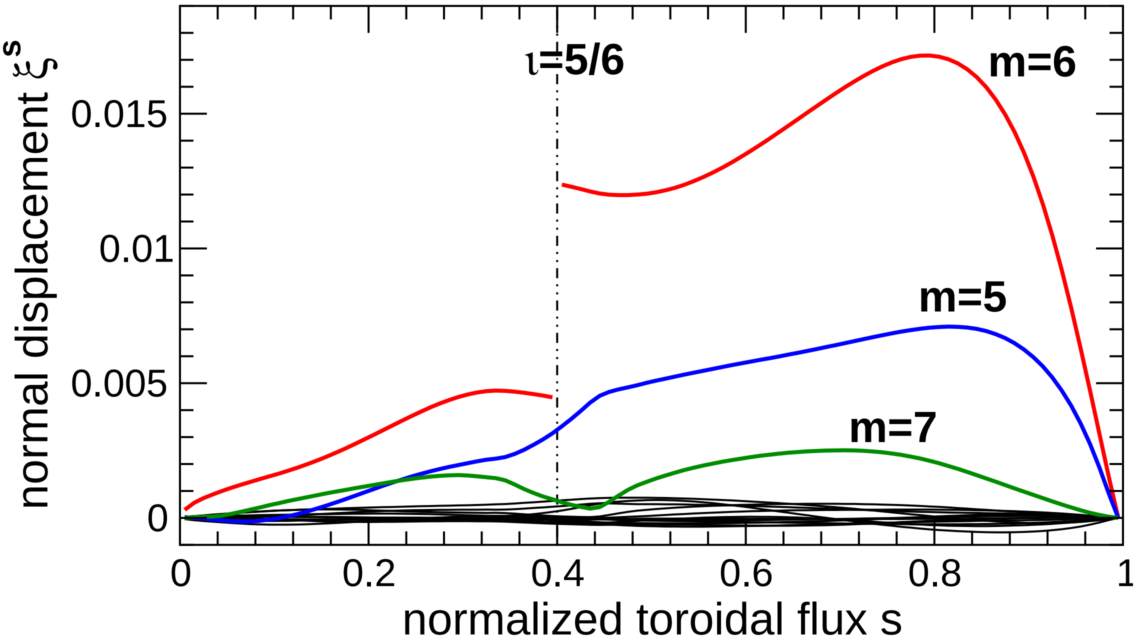

Figure 5: *CAS3D result for the W7-X case of Fig. 2: The dominant normal displacement harmonics versus normalized toroidal flux s, toroidal Fourier index: $n = 5$. The resonant harmonic ($m = 6$, red) jumps at its rational surface (dashed). Non-resonant harmonics (e.g. $m = 5$ and $m = 7$) are continuous everywhere.*

which are used to model islands: the strength of such a surface current can be used to estimate the corresponding island width.

4.1. Applications

ι	PIES	CAS3D
3/5	0.110	0.103
3/6	0.041	0.040
3/7	0.023	0.019
6/9	0.050	0.045

Table I: *Normalized island sizes, $\mathcal{W}/a_{\mathrm{minor}}$, from the PIES and CAS3D codes for the NCSX-type case of Fig. 1 (lowest-order islands, $a_{\mathrm{minor}} = 0.32$ m).*

The augmented CAS3D code was applied to the stellarator cases of Figs. 1 and 2 for a study of the intrinsic islands. This means that Eq. (8) was used with a non-vanishing RHS $\vec{g}$ and homogeneous boundary conditions, $\xi^s(\mathrm{boundary}) \equiv 0$. The surface current on a rational-ι surface which is used to determine an island width is related to the discontinuities of the resonant normal displacement harmonics at the respective resonant surfaces and follows from Eq. (9). In a study of intrinsic islands, the toroidal periodicity of the perturbations must be compatible with the number of field periods of the stellarator.

The result for the NCSX-type case is shown in Fig. 4. The initial fixed-boundary VMEC calculation which is needed to construct the set of surfaces that is examined by CAS3D used the plasma boundary of the fixed-boundary PIES calculation with results in Fig. 1. The CAS3D calculation used 481 radial points and 66 normal displacement harmonics including 24 resonant ones. The perturbation Fourier table included toroidal Fourier indices $n = 3, 6, 9$, and 12, and poloidal Fourier indices $0 \le m \le 34$. The result shows that the resonant harmonics do not vanish interior to their respective resonant surfaces which is a consequence of the mode coupling in general-geometry plasmas. In a cylinder the mode coupling is absent and, therefore, complete shielding prevails at the resonant surfaces [14]. For the lowest-order islands at $\iota = 3/7, 3/6, 3/5$, and $2/3 = 6/9$ the normalized island sizes as computed by the PIES and CAS3D codes have been compared, see Table I. Good agreement has been found.

The result for W7-X is shown in Fig. 5. The low-order rational rotational transform, $\iota = 5/6$, occurs at 40% of the total enclosed toroidal flux. For a reconstruction of the case by VMEC a field-line close to the separatrix, but still giving a *good* magnetic surface in the PIES magnetic field, was chosen as the plasma boundary in a fixed-boundary VMEC calculation. The VMEC surfaces are shown in Fig. 2 (red solid lines) together with the PIES result. The CAS3D calculation used 100 radial intervals and 15 normal displacement harmonics one of them being resonant ($m = 6$, $n = 5$). The perturbation Fourier table included toroidal Fourier indices $n = 0, 5$, and 10, and poloidal Fourier indices up to $m = 9$. Although mode coupling prevents the resonant perturbation harmonic from being completely shielded at the respective resonant surface, $\iota = 5/6$, the shielding is significant. The CAS3D analysis predicts an island width of ≈ 0.029m which is comparable to the PIES result of ≈ 0.027m.

5. Summary

For the W7-X and NCSX stellarators finite-β equilibria with magnetic islands have been obtained with the PIES code. The alternative method to determine islands within ideal MHD uses the concept of perturbed equilibria implemented in the CAS3D code and yields island sizes comparable to the ones given by PIES.

References

[1] REIMAN, A. H. et al., Calculation of three-dimensional MHD equilibria with islands and stochastic regions, Comput. Phys. Commun. **43** (1986) 157.

[2] HAYASHI, T., Ergodization of magnetic surfaces due to finite β effect in a helical system, in *Theory of Fusion Plasmas Chexbres 1988*, volume EUR 12149 EN, page 11, Bologna, 1989, Società Italiana di Fisica.

[3] BOOZER, A. H., Perturbed plasma equilibria, Phys. Plasmas **6** (1999) 831.

[4] NÜHRENBERG, C. et al., Magnetic islands and perturbed plasma equilibria, Phys. Plasmas **10** (2003) 2840.

[5] ZARNSTORFF, M. C. et al., Physics of the compact advanced stellarator NCSX, Plasma Phys. Control. Fusion **43** (2001) A237.

[6] LOTZ, W. et al., Optimization, MHD mode and alpha particle confinement behaviour of Helias equilibria, in *Plasma Physics and Controlled Nuclear Fusion Research 1990*, volume **2** of *Nucl. Fusion Suppl.*, page 603, Vienna, 1991, International Atomic Energy Agency.

[7] HIRSHMAN, S. P. et al., Three-dimensional free boundary calculations using a spectral Green's function method, Comput. Phys. Commun. **43** (1986) 143.

[8] SPITZER, L., The stellarator concept, Phys. Fluids **1** (1958) 253.

[9] HUDSON, S. R. et al., Eliminating islands in high-pressure free-boundary stellarator magnetohydrodynamic equilibrium solutions, Phys. Rev. Lett. **89** (2002) 275003.

[10] ANDREEVA, T., Vacuum magnetic configurations of Wendelstein 7-X, Technical report, MPI f. Plasmaphysik, IPP-Report 3/270, 2002.

[11] DREVLAK, M. et al., PIES free boundary stellarator equilibria with improved initial conditions, Nucl. Fusion **45** (2005) 731.

[12] STRUMBERGER, E., Finite-β magnetic field line tracing for helias configurations, Nucl. Fusion **37** (1997) 19.

[13] PARK, J.-K. et al., Computation of three-dimensional tokamak and spherical torus equilibria, Phys. Plasmas **14** (2007) 052110.

[14] NÜHRENBERG, C. et al., Verification of the CAS3D-perturbed equilibrium code in the cylindrical limit, in *34th EPS Conf. on Contr. Fus. and Plasma Phys. , Warsaw 2007*, Europ. Conf. Abstr., Geneva, 2007, P4.065, Europ. Phys. Soc.